2017

# How should a local regime-switching model be calibrated?

Xin-Jiang He
*University of Wollongong*, xh016@uowmail.edu.au

Song-Ping Zhu
*University of Wollongong*, spz@uow.edu.au

# How should a local regime-switching model be calibrated?


## Abstract

Local regime-switching models are a natural consequence of combining the concept of a local volatility model with that of a regime-switching model. However, even though Elliott et al. (2015) have derived a Dupire formula for a local regime-switching model, its calibration still remains a challenge, primarily due to the fact that the derived volatility function for each state involves all the state price variables whereas only one market price is available for model calibration, and a direct implementation of Elliott et al.'s formula may not yield stable results. In this paper, a closed system for option pricing and data extraction under the classical regime-switching model is proposed with a special approach, splitting one market price into two "market-implied state prices". The success of our approach hinges on the recovery of the two local volatility functions being transformed into an optimal control problem, which is solved through the Tikhonov regularization. In addition, an efficient algorithm is proposed to obtain the optimal solution by iteration. Our numerical experiments show that different shapes of local volatility functions can be accurately and stably recovered with the newly-proposed algorithm, and this algorithm also works quite well with real market data.



## Disciplines

Engineering | Science and Technology Studies

## Publication Details

He, X. & Zhu, S. (2017). How should a local regime-switching model be calibrated?. Journal of Economic Dynamics and Control, 78 149-163.

# How should a local regime-switching model be calibrated?

Xin-Jiang HE [*] Song-Ping ZHU [†]

**Abstract**

Local regime-switching models are a natural consequence of combining the concept of a local volatility model with that of a regime-switching model. However, even though Elliott et al. (2015) have derived a Dupire formula for a local regime-switching model, its calibration still remains a challenge, primarily due to the fact that the derived volatility function for each state involves all the state price variables whereas only one market price is available for model calibration, and a direct implementation of Elliott et al.'s formula may not yield stable results. In this paper, a closed system for option pricing and data extraction under the classical regime-switching model is proposed with a special approach, splitting one market price into two "market-implied state prices". The success of our approach hinges on the recovery of the two local volatility functions being transformed into an optimal control problem, which is solved through the Tikhonov regularization. In addition, an efficient algorithm is proposed to obtain the optimal solution by iteration. Our numerical experiments show that different shapes of local volatility functions can be accurately and stably recovered with the newly-proposed algorithm, and this algorithm also works quite well with real market data.

[*]School of Mathematics and Applied Statistics, University of Wollongong NSW 2522, Australia

[†]Corresponding author. School of Mathematics and Applied Statistics, University of Wollongong NSW 2522, Australia.

**AMS(MOS) subject classification.**

**Keywords.** Local regime-switching model, Closed system, Optimal control problem, Tikhonov regularization.

# 1 Introduction

Despite the great success of the Black-Scholes model (cf. Black and Scholes (1973)), in which the returns of the underlying were assumed to follow a log-normal distribution and a closed-form pricing formula for European options was derived, some of its simplified assumptions made to achieve analytical tractability are inappropriate and may lead to large pricing errors. In particular, one of its main drawbacks is the unrealistic assumption of constant volatility since the implied volatility extracted from market data tends to exhibit a "smile" curve with respect to the strike price (cf. Dumas et al. (1998)), indicating that the assumption of constant volatility needs to be revised. As a result, a number of modifications have been proposed by introducing non-constant volatility in modeling underlying prices so that options can be priced with a model closer to reality.

In the literature, the non-constant volatility models can mainly be divided into two categories, i.e. stochastic volatility and local volatility. The former was investigated by a number of authors, such as Heston (1993) with a CIR (Cox-Ingersoll-Ross) model to describe the volatility dynamic, and Hagan et al. (2002) with a SABR model. Moreover, jump-diffusion dynamics are also combined with stochastic volatility by a number of authors, such as Bates (2000), and Scott (1997). On the other hand, local volatility models were considered by Dupire (1994), Rubinstein (1994), and Derman and Kani (1994), who introduced the concept of taking volatility as a deterministic function of the underlying price and time, the specific form of which can be determined from market data through a model calibration process. There are a number of attractive features of local volatility models (e.g., see Derman et al. (1996), Kamp (2009), Musiela and Rutkowski (2006)). For

example, local volatility models are easy and fast to calibrate since the only source of randomness is the underlying price. Also, the market becomes complete when adopting local volatility models and thus any contingent claim can be perfectly replicated with a portfolio consisting of the underlying and bond only. Most importantly, local volatility models can perfectly match any arbitrage-free set of European option prices. On the other hand, the generated local volatility surface in any local volatility model is actually static, which may yield poor hedging results (cf. Fengler et al. (2003), Hagan et al. (2002)), and thus some hybrid models that combine local volatility and stochastic volatility have been proposed as a result (Choi et al. (2013) and Van der Stoep et al. (2014)).

Recently, another kind of stochastic volatility models, the regime-switching model, is becoming quite popular since it proves to better capture the changing beliefs of investors towards the states of certain financial markets (cf. Hamilton (1990)). It was first introduced by Hamilton (1989) and the volatility in this model can jump between different states controlled by a Markov chain. Its main attraction comes from a lot of empirical evidence, which suggests that the dynamics of the underlying price are better captured by allowing volatility to switch between different states (cf. Chernov et al. (2003), Eraker (2004)). Therefore, it has been introduced to the area of financial derivative pricing and extensively studied by a number of researchers. For example, under regime-switching models, Naik (1993) and Zhu et al. (2012) worked on the valuation problem of European options, while Buffington and Elliott (2002) and Bollen (1998) priced American option contracts. Recently, the regime-switching mechanism has also been introduced into classical stochastic volatility models to form a regime-switching stochastic volatility models. In specific, Elliott et al. (2007) introduced regime-switching into the Heston model with the long-term mean of the volatility process allowed to jump between different states and analytically evaluated volatility swaps, while the option pricing problem under general regime-switching stochastic volatility models was considered in Goutte (2013). Another example is Siu et al. (2008), where the currency options are evaluated under a two-factor

stochastic volatility model with regime-switching.

However, like in the Black-Scholes model, the assumptions of the classical regime-switching model with a constant volatility in each state may also need to be relaxed, in order to better fit to market prices of options. This idea has prompted the development of the so-called local regime-switching model, where the volatility is a deterministic function of the underlying price and time rather than a constant that can switch among different states. Although Elliott et al. (2015) have derived a Dupire equation (denoted by Elliott formula in the following) for the regime-switching model recently, they do not investigate the recovery of local volatility functions from market data, which is what we focus on throughout this paper[1].

In fact, it should be emphasized that there are few empirical studies on regime-switching option pricing models, and it is even unclear on how to calibrate regime-switching models. Therefore, it is necessary to first develop an approach to implement Elliott's formula. In particular, the main two challenges in this model calibration process are a) the derived volatility function for each state involves all the state price variables whereas only one market price is available for model calibration; b) a direct implementation of Elliott et al.'s formula may not yield stable results. Hence, their formula alone does not allow the recovery of local volatility functions, and what will be presented first is a closed system on how to price options in real markets with classical regime-switching models, based on which one market price is split into two market-implied state prices through two financially meaningful equations. Once we have successfully obtained two market-implied state prices, another problem will certainly appear that Elliott formula can not be directly implemented since it may not yield accurate results due to the denominator being directly affected by the second-order derivative of option prices, the problem of which is similar to the case for the implementation of the Dupire formula in the Black-Scholes model (cf. Kamp (2009),

[1]For illustration purpose, we shall focus on discussing the two-state regime-switching model in this paper; the extension to arbitrary but finite number of states should be in principle very similar to what we present here.

Yen and Lai (2014)).

Specifically, under local volatility models, option prices as well as their derivatives can rarely be analytically derived, which implies that numerical approximations for the derivatives have to be made in the evaluation of the local volatility. However, the value of the second-order derivative of the option price with respect to the strike price is usually very small, and its approximation can result in large errors of the obtained local volatility as it appears in the denominator (cf. Kamp (2009), Yen and Lai (2014)). The problem further deteriorates when the approximation of this particular second-order derivative becomes negative, in which case the local volatility model fails as the calculated volatility is no longer a real number. For this reason, two main kinds of approaches have been proposed to solve this problem for the Black-Scholes model.

The first is to express local volatility in terms of a function of implied volatility (cf. Gatheral (2011)) so that the second-order derivative does not soly appear in the denominator, which means that a small error induced on the second-order derivative does not necessarily lead to large errors of the entire volatility surface any more. However, this approach has a shortfall; the implied volatility remains a discontinuous function as a result of only scarce values of strike price and maturities being available in practice. This means that to obtain a local volatility function, one still needs to make necessary interpolation and extrapolation for a set of given data, which is a very difficult task itself with the constraint that no arbitrage opportunities should be introduced in the process of these numerical treatments. Another popular method is to use regularized approach to develop different algorithms so as to stably and accurately recover the local volatility function (cf. Egger and Engl (2005), Jiang et al. (2003)). Having been aware of the advantage of the regularized approach over the implied volatility approach, we will also adopt the regularized approach, and formulate the calibration problem associated with the local regime-switching model into an inverse problem of PDEs (partial differential equations) in this paper. However, it should also be stressed that inverse problems are typically ill posed (cf. Vogel (2002)), and

the situation is even worse in finance since not only option prices available in real markets are discontinuous, but also inadequate option data in terms of strikes and maturities is a serious issue that needs to be dealt with (cf. Coleman et al. (2001), Crepey (2003), De Cezaro et al. (2012), Hofmann and Krämer (2005)). In order to obtain stable results for this inverse problem, it is further transformed into an optimal control problem with the Tikhonov regularization (cf. Tikhonov et al. (2013)). Then, two necessary conditions that the optimal solution should satisfy are derived, based on which a numerical algorithm for iteration is proposed to obtain the optimal solution. Numerical experiments with synthetic are subsequently carried out to show the accuracy and stability of our algorithm, after which the performance of our algorithm is further tested with real market data.

The rest of the paper is organized as follows. In Section 2, we will firstly propose a closed system to price options under the regime-switching model and then the specific steps to split one market price into two market-implied state prices for an option under this system will be introduced. In Section 3, the calibration problem will be formulated into an inverse problem, which is further formed as an optimal control problem and is solved by a Tikhonov regularization approach. Two necessary conditions are also derived so that the numerical algorithm can be developed to find the optimal solution. In Section 4, numerical experiments and market tests for our algorithm are presented, followed by some concluding remarks given in the last section.

# 2 A closed system for calibration

In this section, a closed system should be established first for option pricing under regime-switching models with the constant volatility in each state, based on which how to split one market price of a European option into two market-implied state prices will be illustrated.

Let $S_t$ be the price process of the underlying asset, then it follows a two-state regime-

switching model under the risk-neutral measure as

$$\frac{dS_t}{S_t} = rdt + \sigma_{X_t}(S,t)dW_t, \tag{2.1}$$

where $W_t$ is a Brownian motion independent of $X_t$ and $r$ represents the risk-free interest rate. In addition, $X_t$ is a two-state Markov chain, which jumps between two states, i.e., $X_t \in \{(1,0)', (0,1)'\}$. Here, $v'$ denotes the transpose of the vector $v$. If we define $\bar{\sigma}(S,t) = (\sigma_1(S,t), \sigma_2(S,t))'$ and let $< \cdot, \cdot >$ be the inner product of two vectors, $\sigma_{X_t}(S,t)$ can be expressed as

$$\sigma_{X_t}(S,t) =< \bar{\sigma}(S,t), X_t > . \tag{2.2}$$

Moreover, the transition between the two states follows a Poisson process as

$$P(t_{ij} > t) = e^{-\lambda_{ij}t}, i, j = 1, 2, \ i \neq j.$$

Here $\lambda_{ij}$ is the transition rate from State $i$ to $j$, and $t_{ij}$ is the time spent in State $i$ before transferring to State $j$.

It should be noted that there can be different ways to price options under this model. One approach is to assume that the market state is observable and the price of an option is the corresponding state price. However, it is usually difficult to determine which state the underlying asset price belongs to in practice, and thus it is more reasonable that the states of a financial market are treated as unobservable. The justification of the latter approach lies in the stochastic nature of the volatility under a regime-switching model. In fact, for any stochastic volatility model, the current value of stochastic volatility is an unknown variable which needs to be estimated from real market data together with other model parameters. Such an "unobservable" nature has been discussed in the literature (cf. Aı et al. (2007)). Due to the existence of Markov chain, regime-switching models are a special kind of stochastic volatility models and thus the volatility in any regime-switching model,

together with the status of the regime the market is currently in, should all be assumed unobservable, as we do in this paper.

Some people may argue that we are not able to obtain option prices without knowing the current state. However, this does not have to be true because when pricing an option, the probability of the underlying price being in each state at the current time should be known and be regarded as a model parameter. In this case the market price should be the expectation of the two state prices. Specifically, if we let $C_1$ and $C_2$ be the two state prices of a European option, and make $\pi$ the probability of the underlying price that stays at the regime 1 at the current time (obviously the probability for the regime 2 is $1-\pi$), then it is reasonable to argue that the option price $C$ should be

$$C = C_1\pi + C_2(1-\pi).$$

On the other hand, it is not clear how a regime switching model should be calibrated from a given set of data. Unlike the B-S model, where only the volatility needs to be estimated, the initial state probability, with which the state probability at any later time can be calculated, should be another parameter that needs to be determined through market data, apart from the two constant volatilities and two transition rates, when empirical studies are conducted for the classical regime-switching model. This can be analogous to the stochastic volatility model, in which the initial volatility level needs to be estimated too. In this case model prices can be calculated through $C_1\pi + C_2(1-\pi)$ and all model parameters can be estimated through some global optimization approaches by minimizing the "distance" between market prices and corresponding model prices, which can be done similarly as a lot of existing empirical studies (cf. Bakshi et al. (1997), Chan et al. (1992)).

Considering all the discussion above, the closed system for option pricing under classical regime-switching models with the constant volatility in each state has already been set up.

However, this is not enough when we take into account the local regime-switching model

since both of two state prices need to be used to recover the local volatility of any state in this model, which implies that one market price of a European option should be split into two corresponding state prices. Therefore, if we still assume $C_1$ and $C_2$ be the two market-implied state prices corresponding to the market price $C^{market}$, we still need an extra equation to determine $C_1$ and $C_2$, apart from the following equation

$$C^{market} = C_1\pi + C_2(1-\pi). \tag{2.3}$$

In fact, the choice for such an equation is quite free as long as this equation always holds when the regime-switching model degenerates to the Black-Scholes model.

One method that we believe is reasonable is that first of all, $\lambda_{12}$ and $\lambda_{21}$ and the two constant volatilities as well as the initial state probability are estimated with historical underlying and option data (cf. Janczura and Weron (2012), Mitra and Date (2010)), with which two state prices $V_1$ and $V_2$ can be worked out. It should be remarked that the two market-implied state prices $C_1$ and $C_2$ does not equal to the calculated $V_1$ and $V_2$ since $V_1$ and $V_2$ are obtained based on the assumption that the volatility in each state is constant. We then treat $V_1$ and $V_2$ as an approximation of $C_1$ and $C_2$ respectively and the relationship between them is imposed to serve as another equation

$$f(V_1, V_2, C_1, C_2) = 0. \tag{2.4}$$

The intuition behind such an approximation is that extracting parameters from real market data under classical regime-switching models has already made the model prices $C^{model}$ calculated with these parameters very close to real market prices, and thus the corresponding state prices should also be a good approximation for the market-implied state prices. In this sense, one of the simplest examples is

$$(V_1 - V_2) - (C_1 - C_2) = 0, \tag{2.5}$$

the choice of which is based on two main reasons. One is that it obviously meets the requirement that it always holds when the regime-switching model degenerates to the Black-Scholes model since in this case $V_1 = V_2$ and $C_1 = C_2$. Moreover, it is obvious that the biases between market prices and classical regime-switching model prices are caused by the difference between each state price of local regime-switching models and that of classical regime-switching models, and we make a reasonable assumption that the amount of these biases contributed by each state is the same.

With Equation (2.3) and Equation (2.4), it is not difficult to find that given one set of market prices, we can split them into two sets of market-implied state prices. Therefore, we are now ready to proceed to the calibration problem, which will be presented in the next section.

# 3 Calibration problem

In this section, a well-posed inverse problem for the calibration of local regime-witching models will be pointed out, and then a Tikhonov regularization approach will be introduced to recover smooth local volatility functions with the two sets of market-implied state prices obtained in the last section. Afterwards, two necessary conditions can be derived in order to reach the optimal solution, followed by the numerical algorithm showing the procedure of iteration to obtain the recovered local volatility functions.

## 3.1 An inverse problem

In this subsection, recovering the local volatility functions will firstly be formed into an ill-posed inverse problem, which will be further transformed into a well-posed inverse problem, before it can be properly solved.

If we let $V_1(S, t; K, T)$ and $V_2(S, t; K, T)$ be European call option prices for State 1 and State 2 respectively with $K$ being the strike price and $T$ being the expiry time, a

system of coupled Black-Scholes equations for the option prices can be derived according to Buffington and Elliott (2002)

$$\begin{cases} \dfrac{\partial V_1}{\partial t} + \dfrac{1}{2}\sigma_1^2 S^2 \dfrac{\partial^2 V_1}{\partial S^2} + rS\dfrac{\partial V_1}{\partial S} - rV_1 - \lambda_{12}(V_1 - V_2) = 0,\ S > 0,\ t \in [0,T], \\ V_1(S,T) = \max(S-K,0), \\ V_1(0,t) = 0, \end{cases} \tag{3.1}$$

$$\begin{cases} \dfrac{\partial V_2}{\partial t} + \dfrac{1}{2}\sigma_2^2 S^2 \dfrac{\partial^2 V_2}{\partial S^2} + rS\dfrac{\partial V_2}{\partial S} - rV_2 - \lambda_{21}(V_2 - V_1) = 0,\ S > 0,\ t \in [0,T], \\ V_2(S,T) = \max(S-K,0), \\ V_2(0,t) = 0. \end{cases} \tag{3.2}$$

Given the two sets of market-implied state prices $V_1^*(S_0, t_0; K, T)$ and $V_2^*(S_0, t_0; K, T)$ with different maturities and strike prices at time $t_0$, we want to recover the local volatility functions $\sigma_1(S,t)$ and $\sigma_2(S,t)$ for the two states from these market state prices, which formulate the following inverse problem.

**Problem 1** *Find the two functions $\sigma_1(S,t)$ and $\sigma_2(S,t)$ such that the solutions to the coupled PDE system (3.1) and (3.2), $V_1(S_0, t_0; K, T)$ and $V_2(S_0, t_0; K, T)$, satisfy the following two equations*

$$\begin{aligned} V_1(S_0, t_0; K, T) &= V_1^*(S_0, t_0; K, T), \\ V_2(S_0, t_0; K, T) &= V_2^*(S_0, t_0; K, T), \end{aligned}$$

*respectively for all $T$ and $K$.*

Unfortunately, it should be noted that Problem 1 is not well-posed (cf. Rebonato (2005)) since the variables of the coupled PDE system (3.1) and (3.2) are $S$ and $t$, whereas $V_1^*(S_0, t_0; K, T)$ and $V_2^*(S_0, t_0; K, T)$ are observed with respect to $K$ and $T$ at a particular time $t_0$ and underlying price $S_0$. Thereby, alternative ways should be found to obtain the

two local volatility functions. With the help of Elliott et al. (2015), in which a Dupire equation for the regime-switching model is derived, the coupled PDE system (3.1) and (3.2) is established with new variables $K$ and $T$ as

$$\begin{cases} \dfrac{\partial V_1}{\partial T} - \dfrac{1}{2}\sigma_1^2(K,T)K^2\dfrac{\partial^2 V_1}{\partial K^2} + rK\dfrac{\partial V_1}{\partial K} - \lambda_{12}V_1 + \lambda_{21}V_2 = 0,\ K > 0,\ T \geq t_0, \\ V_1(K,t_0) = \max(S_0 - K, 0), \\ V_1(0,T) = S_0, \end{cases} \tag{3.3}$$

$$\begin{cases} \dfrac{\partial V_2}{\partial T} - \dfrac{1}{2}\sigma_2^2(K,T)K^2\dfrac{\partial^2 V_2}{\partial K^2} + rK\dfrac{\partial V_2}{\partial K} - \lambda_{21}V_2 + \lambda_{12}V_1 = 0,\ K > 0,\ T \geq t_0, \\ V_2(K,t_0) = \max(S_0 - K, 0), \\ V_2(0,T) = S_0. \end{cases} \tag{3.4}$$

In theory, it is quite easy to work out the local volatility by simply differentiating the state prices once with respect to strike and expiry respectively, and twice with respect to the strike. However, the computation may not be stable since it involves the second-order derivative with respect to the strike and we can not guarantee that the variance be positive. Furthermore, the state prices are discontinuous and the numerical differentiation requires interpolation and extrapolation, which can affect the accuracy of the obtained local volatility. Therefore, another inverse problem should be formulated as summarized below. In this newly formulated problem, we have simplified the solution procedure for the inverse problem by assuming that the volatility be independent of time, in order to focus on the core issue for this paper, i.e., to illustrate how a local regime-switching model can be calibrated. Of course, as a progressive approach to tackle the complexity arisen from the multi-dimensionality of an inverse problem, such kind of simplified assumptions has already been adopted in calibrating local Black-Scholes model with real market data (e.g., Bouchouev and Isakov (1997)).

**Problem 2** *Given the fixed maturity $T$, find the two functions $\sigma_1(K)$ and $\sigma_2(K)$ such that*

*the solution to the coupled PDE system (3.3)-(3.4), $V_1(K)$ and $V_2(K)$, satisfy the following two equations*

$$\begin{aligned} V_1(K,T) &= V_1^*(K), \\ V_2(K,T) &= V_2^*(K), \end{aligned}$$

*respectively for all $K$.*

Here, for simplicity, we denote

$$\begin{aligned} V_i(K,T) &= V_i(S_0,t_0;K,T), \\ V_i^*(K) &= V_i^*(S_0,t_0;K,T), \end{aligned}$$

for $i = 1, 2$.

By now, we have already formed a well-posed inverse problem for the recovery of local volatility functions in the sense that the market data is observed with respect to the strike price $K$ and the maturity $T$, which are exactly the same as the variables in the PDE system (3.3)-(3.4). This has paved the way for us to solve this problem, which is illustrated in the next subsection.

## 3.2 Tikhonov regularization

In this subsection, Tikhonov regularization will be used to solve Problem 2. The motivation for us to adopt this particular regularization technique is that it allows us to obtain stable solutions to optimal control problems. In particular, the two local volatility functions in regime-switching models should be determined simultaneously so that the following cost

function is minimized

$$J(\sigma_1,\sigma_2)=\frac{\delta}{2}\int_0^{+\infty}(\frac{\partial\sigma_1}{\partial K})^2+(\frac{\partial\sigma_2}{\partial K})^2dK+\frac{1}{2}\int_0^{+\infty}[V_1(K,\tau_0)-V_1^*(K)]^2+[V_2(K,\tau_0)-V_2^*(K)]^2dK, \tag{3.5}$$

where $\tau = T-t$, and $\delta$ is called the Tikhonov regularization parameter. Therefore, Problem 2 derived in the last subsection is now turned into an optimal control problem that we should find $\bar{\sigma}_1(K)$ and $\bar{\sigma}_2(K)$ such that

$$J(\bar{\sigma}_1,\bar{\sigma}_2)=\inf_{\sigma_1,\sigma_2\in A}J(\sigma_1,\sigma_2), \tag{3.6}$$

where $A=\{\sigma\in C(R)|\frac{\partial\sigma}{\partial K}\in L^2(R)\}$.

Therefore, recovering the two local volatility functions reduces to solve this optimal control problem, for which we will derive two necessary conditions. If we assume $\bar{\sigma}_1(K)$ and $\bar{\sigma}_2(K)$ be the solution of the optimal control problem (3.6), it is clear that for any $h\in A$, both of the following two functions, i.e. $J(\bar{\sigma}_1+\lambda h,\bar{\sigma}_2)$ and $J(\bar{\sigma}_1,\bar{\sigma}_2+\lambda h)$, reach their minimum when $\lambda=0$, which implies

$$\frac{d}{d\lambda}J(\bar{\sigma}_1+\lambda h,\bar{\sigma}_2)|_{\lambda=0}=0,\quad \frac{d}{d\lambda}J(\bar{\sigma}_1,\bar{\sigma}_2+\lambda h)|_{\lambda=0}=0. \tag{3.7}$$

With

$$\frac{d}{d\lambda}\big[(\frac{\partial(\bar{\sigma}_i+\lambda h)}{\partial K})^2\big]\big|_{\lambda=0}=\Big\{2\frac{\partial(\bar{\sigma}_i+\lambda h)}{\partial K}\times\frac{d}{d\lambda}\big[\frac{\partial(\bar{\sigma}_i+\lambda h)}{\partial K}\big]\Big\}\Big|_{\lambda=0}=2\frac{\partial\bar{\sigma}_i}{\partial K}\frac{\partial h}{\partial K},$$

and

$$\begin{aligned}\frac{d}{d\lambda}\big\{[V_i(K,\tau;\bar{\sigma}_i+\lambda h)-V_i^*(K)]^2\big\}\big|_{\lambda=0} &= \Big\{2[V_i(K,\tau;\bar{\sigma}_i+\lambda h)-V_i^*(K)]\times\frac{dV_i(K,\tau;\bar{\sigma}_i+\lambda h)}{d\lambda}\Big\}\Big|_{\lambda=0}\\ &= [V_1(K,\tau)-V_1^*(K)]\xi_i(K,\tau),\end{aligned}$$

where $\xi_i(K,\tau) = \frac{dV_i(K,\tau;\bar{\sigma}_1+\lambda h,\bar{\sigma}_2)}{d\lambda}|_{\lambda=0}$, $\eta_i(K,\tau) = \frac{dV_i(K,\tau;\bar{\sigma}_1,\bar{\sigma}_2+\lambda h)}{d\lambda}|_{\lambda=0}$ for $i = 1, 2$, Equation (3.7) can certainly yield

$$\delta \int_0^{+\infty} \frac{\partial \bar{\sigma}_1}{\partial K}\frac{\partial h}{\partial K}dK + \int_0^{+\infty} [V_1(K,\tau_0) - V_1^*(K)]\xi_1(K,\tau_0) + [V_2(K,\tau_0) - V_2^*(K)]\xi_2(K,\tau_0)dK = 0, \tag{3.8}$$

$$\delta \int_0^{+\infty} \frac{\partial \bar{\sigma}_2}{\partial K}\frac{\partial h}{\partial K}dK + \int_0^{+\infty} [V_1(K,\tau_0) - V_1^*(K)]\eta_1(K,\tau_0) + [V_2(K,\tau_0) - V_2^*(K)]\eta_2(K,\tau_0)dK = 0, \tag{3.9}$$

To work out the necessary condition (3.8), what we should do first is to calculate the two functions $\xi_1(K,\tau)$ and $\xi_2(K,\tau)$. In fact, $V_i(K,\tau;\bar{\sigma}_1+\lambda h,\bar{\sigma}_2), i = 1, 2$ should satisfy the PDE in (3.3) and (3.4), respectively, except that $\sigma_1$ is replaced by $\bar{\sigma}_1 + \lambda h$. Therefore, by taking the derivative on both sides of the coupled PDEs governing $V_i(K,\tau;\bar{\sigma}_1 + \lambda h, \bar{\sigma}_2), i = 1, 2$ with respect to $\lambda$ and then setting $\lambda = 0$, we can find that $\xi_1(K,\tau)$ and $\xi_2(K,\tau)$ satisfy the following coupled PDE system

$$\begin{aligned} L_1\xi_1 &\triangleq \frac{\partial \xi_1}{\partial \tau} - \frac{1}{2}\sigma_1^2 K^2 \frac{\partial^2 \xi_1}{\partial K^2} + rK\frac{\partial \xi_1}{\partial K} - \lambda_{12}\xi_1 + \lambda_{21}\xi_2 = h\sigma_1 K^2 \frac{\partial^2 V_1}{\partial K^2}, \\ L_2\xi_2 &\triangleq \frac{\partial \xi_2}{\partial \tau} - \frac{1}{2}\sigma_2^2 K^2 \frac{\partial^2 \xi_2}{\partial K^2} + rK\frac{\partial \xi_2}{\partial K} - \lambda_{21}\xi_2 + \lambda_{12}\xi_1 = 0, \end{aligned}$$

with the initial conditions

$$\xi_1|_{\tau=0} = 0, \quad \xi_2|_{\tau=0} = 0.$$

It should be remarked here that it is very difficult to directly figure out $\xi_1(K,\tau)$ and $\xi_2(K,\tau)$ from the above coupled PDEs as the existence of the unknown function $h$, and thus we have to find an alternative way. Now, we let $L = (L_1, L_2)$, and denote $L^* = (L_1^*, L_2^*)$ as the adjoint operator of $L$ (cf. Elliott et al. (2015)). We further assume $\phi_1$ and $\phi_2$ be the solution to the adjoint PDEs

$$L_1^*\phi_1 \triangleq -\frac{\partial \phi_1}{\partial \tau} - \frac{\partial^2(\frac{1}{2}\sigma_1^2 K^2\phi_1)}{\partial K^2} - \frac{\partial(rK\phi_1)}{\partial K} - \lambda_{12}\phi_1 + \lambda_{12}\phi_2 = 0, \tag{3.10}$$

$$L_2^*\phi_2 \triangleq -\frac{\partial \phi_2}{\partial \tau} - \frac{\partial^2(\frac{1}{2}\sigma_2^2 K^2\phi_2)}{\partial K^2} - \frac{\partial(rK\phi_2)}{\partial K} - \lambda_{21}\phi_2 + \lambda_{21}\phi_1 = 0, \tag{3.11}$$

with the terminal conditions given by

$$\phi_1|_{\tau=\tau_0} = V_1(K,\tau_0) - V_1^*(K), \quad \phi_2|_{\tau=\tau_0} = V_2(K,\tau_0) - V_2^*(K).$$

Then, it is not difficult to obtain

$$\begin{aligned} Z &\triangleq \int_0^{\tau_0}\int_0^{+\infty} (\phi_1 L_1\xi_1 + \phi_2 L_2\xi_2) - (\xi_1 L_1^*\phi_1 + \xi_2 L_2^*\phi_2)dKd\tau, \\ &= \int_0^{\tau_0}\int_0^{+\infty} (\phi_1\frac{\partial\xi_1}{\partial\tau} + \xi_1\frac{\partial\phi_1}{\partial\tau}) + (\phi_2\frac{\partial\xi_2}{\partial\tau} + \xi_2\frac{\partial\phi_2}{\partial\tau})dKd\tau \\ &+ \int_0^{\tau_0}\int_0^{+\infty} (\phi_1\hat{L}_1\xi_1 + \phi_2\hat{L}_2\xi_2) - (\xi_1\hat{L}_1^*\phi_1 + \xi_2\hat{L}_2^*\phi_2)dKd\tau, \end{aligned} \tag{3.12}$$

where $\hat{L}(=(\hat{L}_1,\hat{L}_2))$ and $\hat{L}^*(=(\hat{L}_1^*,\hat{L}_2^*))$ are derived by removing the derivative with respect to $\tau$ in $L$ and $L^*$ respectively. As a result, $\hat{L}^*$ is also the adjoint operator of $\hat{L}$ with respect to $K$, which can lead to

$$< \hat{L}\xi, \phi >=< \xi, \hat{L}^*\phi >, \tag{3.13}$$

according to the property of adjoint operators with $\xi = (\xi_1,\xi_2)$ and $\phi = (\phi_1,\phi_2)$. This implies

$$\int_0^{+\infty} (\phi_1\hat{L}_1\xi_1 + \phi_2\hat{L}_2\xi_2) - (\xi_1\hat{L}_1^*\phi_1 + \xi_2\hat{L}_2^*\phi_2)dK = 0. \tag{3.14}$$

Therefore, Equation (3.12) can be further simplified as

$$\begin{aligned} Z &= \int_0^{+\infty}\int_0^{\tau_0} (\phi_1\frac{\partial\xi_1}{\partial\tau} + \xi_1\frac{\partial\phi_1}{\partial\tau}) + (\phi_2\frac{\partial\xi_2}{\partial\tau} + \xi_2\frac{\partial\phi_2}{\partial\tau})d\tau dK, \\ &= \int_0^{+\infty} \xi_1\phi_1|_0^{\tau_0} + \xi_2\phi_2|_0^{\tau_0} dK, \\ &= \int_0^{+\infty} [V_1(K,\tau_0) - V_1^*(K)]\xi_1(K,\tau_0) + [V_2(K,\tau_0) - V_2^*(K)]\xi_2(K,\tau_0)dK, \end{aligned} \tag{3.15}$$

the last step of which is obtained by the substitution of the initial condition for $\xi$ and the terminal condition for $\phi$. On the other hand, $Z$ can be calculated directly through its

definition as

$$Z = \int_0^{\tau_0}\int_0^{+\infty}(\phi_1 L_1\xi_1+\phi_2 L_2\xi_2)-(\xi_1 L_1^*\phi_1+\xi_2 L_2^*\phi_2)dKd\tau = \int_0^{\tau_0}\int_0^{+\infty}\phi_1 h\bar{\sigma}_1 K^2\frac{\partial^2 V_1}{\partial K^2}dKd\tau, \tag{3.16}$$

since $L_1\xi_1 = h\sigma_1 K^2\dfrac{\partial^2 V_1}{\partial K^2}$, $L_2\xi_2 = 0$, $L_1^*\phi_1 = 0$, and $L_2^*\phi_2 = 0$. Thereby, Combining Equation (3.8), (3.15) and (3.16) yields

$$\delta\int_0^{+\infty}\frac{\partial\bar{\sigma}_1}{\partial K}\frac{\partial h}{\partial K}dK + \int_0^{\tau_0}\int_0^{+\infty}\phi_1 h\bar{\sigma}_1 K^2\frac{\partial^2 V_1}{\partial K^2}dKd\tau = 0, \tag{3.17}$$

which should hold for any $h \in A$. This demonstrates that $\bar{\sigma}_1$ is the weak solution to the following equation

$$-\delta\frac{\partial^2\bar{\sigma}_1}{\partial K^2} + \int_0^{\tau_0}\phi_1\bar{\sigma}_1 K^2\frac{\partial^2 V_1}{\partial K^2}d\tau = 0. \tag{3.18}$$

In a similar fashion, another necessary condition (3.9) for $\bar{\sigma}_2$ can also be written in a simpler form

$$-\delta\frac{\partial^2\bar{\sigma}_2}{\partial K^2} + \int_0^{\tau_0}\phi_2\bar{\sigma}_2 K^2\frac{\partial^2 V_2}{\partial K^2}d\tau = 0. \tag{3.19}$$

By now, we have obtained the optimality conditions for our optimal control problem (3.6), and thus the problem of recovering the two local volatility functions is now equivalent to finding the solutions of $\phi_i, i = 1, 2$ to the coupled PDEs (3.10) and (3.11) so that $\bar{\sigma}_1$ and $\bar{\sigma}_2$ are solutions to Condition (3.18) and (3.19) respectively. Hence, in the next subsection, a numerical algorithm will be designed to find the optimal solution.

## 3.3 Numerical algorithm

In this subsection, an algorithm is established to obtain the optimal solution to the optimal control problem (3.6). It should be noticed that the algorithm involves solving a system of equation (3.3)-(3.4), (3.10)-(3.11) and (3.18)-(3.19).

Specifically, the semi-infinite operating domain is truncated into a bounded one as

$$\tau \in [0, \tau_0], \quad K \in [0, 2S_0], \tag{3.20}$$

where $S_0$ is the underlying price at $\tau_0$. Let $d\tau$ and $dK$ be the step size in the time direction and the space direction respectively with $N_1 = \dfrac{2S_0}{dK}, N_2 = \dfrac{\tau_0}{d\tau}$, and thus the truncated domain $[0, 2S_0] \times [0, \tau_0]$ is discretized uniformly as

$$\begin{aligned} K_n &= (n-1)\frac{2S_0}{N_1}, \quad n = 1, 2...N_1 + 1, \\ \tau_m &= (m-1)\frac{\tau_0}{N_2}, \quad m = 1, 2...N_2 + 1. \end{aligned}$$

We also denote the functions at $j$-th step iteration as $\bar{\sigma}_{i,j}, V_{i,j}, \phi_{i,j}, i = 1, 2$. Then, given two sets of market-implied state prices, we are now ready to present the iteration procedure.

1. Let $j = 0$. The value of a tolerance parameter $\epsilon$ used to control the convergence of the iteration should be set. Also, initial guesses for the volatility functions $\sigma_{i,0}, i = 1, 2$, need to be chosen.

2. Two sets of option prices $V_{i,j}(K, \tau), i = 1, 2$, can be calculated through PDEs (3.3)-(3.4) corresponding to $\sigma_{i,j}, i = 1, 2$, with an implicit discretization as

$$\begin{aligned} \frac{V_{1,j}^{n,m+1} - V_{1,j}^{n,m}}{d\tau} &- \frac{(\sigma_{1,j}^n)^2 (K_n)^2 [V_{1,j}^{n+1,m+1} - 2V_{1,j}^{n,m+1} + V_{1,j}^{n-1,m+1}]}{2(dK)^2} \\ &- rK_n \frac{V_{1,j}^{n+1,m+1} - V_{1,j}^{n-1,m+1}}{2dK} - \lambda_{12} V_{1,j}^{n,m+1} + \lambda_{21} V_{2,j}^{n,m+1} = 0, \end{aligned}$$

   and

$$\begin{aligned} \frac{V_{2,j}^{n,m+1} - V_{2,j}^{n,m}}{d\tau} &- \frac{(\sigma_{2,j}^n)^2 (K_n)^2 [V_{2,j}^{n+1,m+1} - 2V_{2,j}^{n,m+1} + V_{2,j}^{n-1,m+1}]}{2(dK)^2} \\ &- rK_n \frac{V_{2,j}^{n+1,m+1} - V_{2,j}^{n-1,m+1}}{2dK} - \lambda_{21} V_{2,j}^{n,m+1} + \lambda_{12} V_{1,j}^{n,m+1} = 0. \end{aligned}$$

3. With $\bar{\sigma}_{i,j}, i = 1, 2$, and the obtained $V_{i,j}(K, \tau_0), i = 1, 2$, in Step 2, $\phi_{i,j}, i = 1, 2$, can be calculated by solving PDEs (3.10)-(3.11) with an implicit discretization, which is similar to that in step 2 and thus the scheme is omitted.

4. By making use of $V_{i,j}(K, \tau_0), i = 1, 2$, and $\phi_{i,j}, i = 1, 2$, obtained in Step 2 and 3 respectively, the updated local volatility functions $\bar{\sigma}_{i,j+1}, i = 1, 2$, can be derived by solving the coupled ordinary differential equations (3.18)-(3.19). It should be noted that the integration in the two equations can be carried out with the trapezoidal rule, which is given as

$$\begin{aligned} W_{i,j}^n &\triangleq \int_0^{\tau_0} \phi_{i,j}\bar{\sigma}_{i,j}K^2\frac{\partial^2 V_1}{\partial K^2}\tau, \\ &= \frac{d\tau}{2}\sum_{m=1}^{N_2}[\phi_{i,j}^{n,m}\sigma_{i,j}^n(K_n)^2\frac{V_{i,j}^{n+1,m} - 2V_{i,j}^{n,m} + V_{i,j}^{n-1,m}}{(dK)^2} \\ &+ \phi_{i,j}^{n,m+1}\sigma_{i,j}^n(K_n)^2\frac{V_{i,j}^{n+1,m+1} - 2V_{i,j}^{n,m+1} + V_{i,j}^{n-1,m+1}}{(dK)^2}], \end{aligned}$$

for $i = 1, 2$. In addition, to make the iteration smoother, we introduce a "false" time $\theta$ in solving the two equations. The algorithm is provided in the following

$$\frac{\sigma_{i,j+1}^n - \sigma_{i,j}^n}{\theta} - \delta\frac{\sigma_{i,j}^{n+1} - 2\sigma_{i,j}^n + \sigma_{i,j}^{n-1}}{(dK)^2} + W_{i,j}^n = 0, \tag{3.21}$$

for $i = 1, 2$.

5. If

$$||\sigma_{1,j+1} - \sigma_{1,j}|| + ||\sigma_{2,j+1} - \sigma_{2,j}|| < \epsilon, \tag{3.22}$$

then we let $\bar{\sigma}_i = \sigma_{i,j+1}, i = 1, 2$, and stop the iteration. Otherwise, set $j = j + 1$ and go back to Step 2.

After the algorithm is designed, a natural question is how it performs and whether the recovered volatility functions are accurate. Numerical experiments will be presented in the

next section.

# 4 Numerical experiments and market tests

In this section, numerical experiments are firstly conducted to show the accuracy and the stability of our numerical algorithm, and then the performance of our approach is further tested with real market data.

## 4.1 Accuracy tests

In this subsection, results of numerical experiments are presented to realize the designed algorithm in the last section. In order to demonstrate the accuracy of the algorithm, we carry out tests with exact solutions of the two volatility functions. To be more specific, the two "true" volatility functions denoted by $\sigma_i^*(S), i = 1, 2$, are pre-set, through which two sets of state prices $V_i(S_0, t_0; K_n, T), i = 1, 2$, can be generated with the coupled PDE system (3.1)-(3.2). Afterwards, we treat $V_i(S_0, t_0; K_n, T), i = 1, 2$ as market state prices, i.e.

$$V_i^*(K_n) = V_i(S_0, t_0; K_n, T), \quad i = 1, 2, \tag{4.1}$$

which will be used to recover the volatility functions through our algorithm.

In fact, these tests can be viewed as a pseudo-empirical study, because they were conducted in such a way that a time series of discrete data is generated from a stochastic process with two given volatility functions. Then we tried to see if we could recover the volatility function using the proposed algorithm as an inverse problem. When a hierarchy of given test functions is employed to go through these tests, starting from the simplest constant functions, they are the necessary conditions to ensure that the proposed algorithm is able to cope with much more complicated volatility functions to be recovered from real market data, as any complicated function can be somewhat viewed as a decomposition of

these simple functions.

Three test volatility functions were chosen in order to show that our algorithm is able to recover different shapes of volatility curve. In all these tests, model parameters were set to be

$$\begin{aligned} S_0 &= 10,\ t_0 = 0,\ r = 0.05,\ T = 1,\ \lambda_{12} = 0.1,\ \lambda_{21} = 0.2,\ N_1 = 30,\ N_2 = 50, \\ \delta &= 0.2,\ \theta = 10^{-3},\ \epsilon = 5 * 10^{-12}. \end{aligned}$$

In the first experiment, we start with the lowest order of test function in the hierarchy of the test functions, i.e., with the volatility being "flat" as

$$\sigma_1(S) = 0.4, \quad \sigma_2(S) = 0.2. \tag{4.2}$$

Of course, this does not mean that the volatility function to be recovered in practice will be of such a simple form. But, if the designed algorithm is even unable to recover such simplest form of local volatility functions, this algorithm can never be trusted and should certainly not be adopted for real markets. In other words, this is a necessary step, as the most fundamental function in the hierarchy of test functions to be tested, in order to know how accurately our algorithm can "recover" the true volatility functions in a local regime switching model. Since we don't know the specific forms of the volatility functions in reality, more complicated test functions will be used to gain confidence on the reliability and accuracy of the proposed algorithm to eventually employed to recover volatility functions when real market data are used.

The recovery results for this are shown in Figure 1. What we can see from Figure 1 is that with the initial guess of 0.35 for State 1 volatility and 0.15 for State 2 volatility respectively, the two recovered volatility functions are quite fit to the "true" pre-specified ones with errors only in the order of $10^{-8}$, which is rather satisfactory.

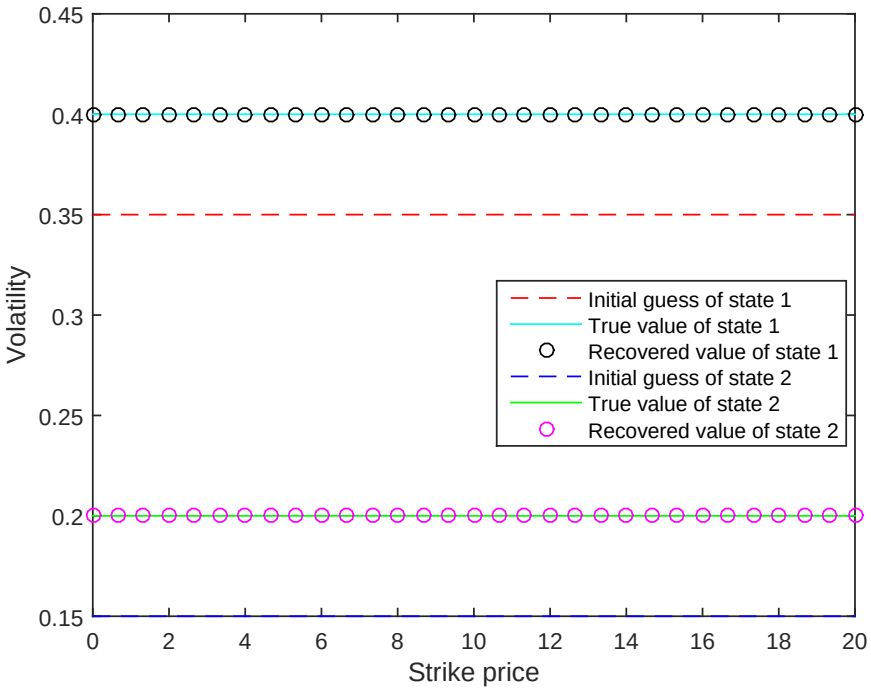


Figure 1: Recovery of the flat-shape volatility

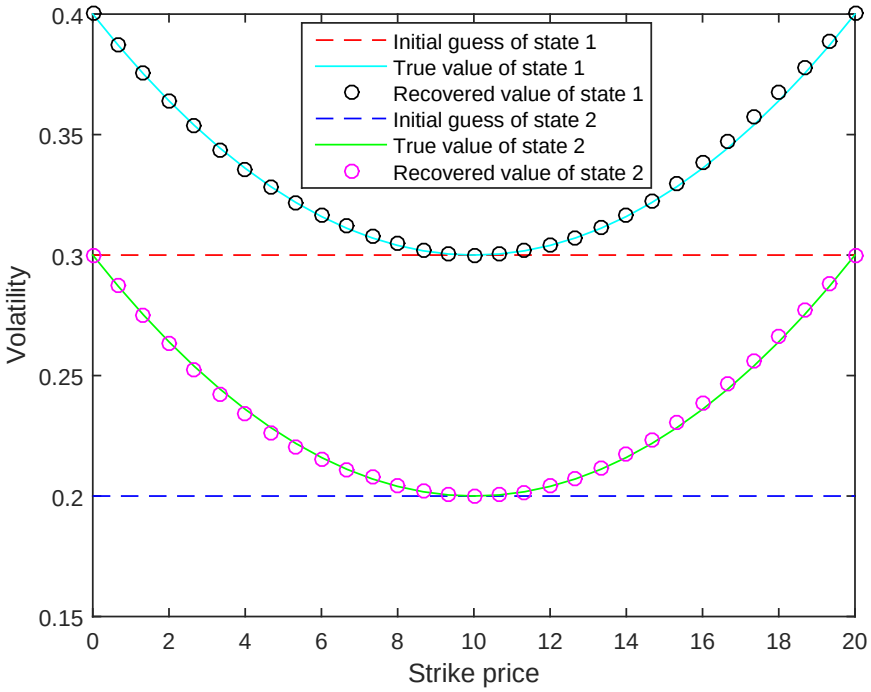


Figure 2: Recovery of the smile-shape volatility

When the shape of the true volatility functions is no longer flat, but exhibits a "smile" curve, which is a common phenomenon observed in real markets (cf. Dumas et al. (1998)), we also try to recover them using our algorithm and these results are shown in Figure 2. In this case, the two "true" volatility functions are

$$\sigma_1(S) = 0.3 + \frac{(S-10)^2}{1000}, \quad \sigma_2(S) = 0.2 + \frac{(S-10)^2}{1000}. \tag{4.3}$$

It is clear that with initial guesses being two flat lines, our algorithm is still able to provide quite accurate results of recovery with errors in the order of $10^{-4}$.

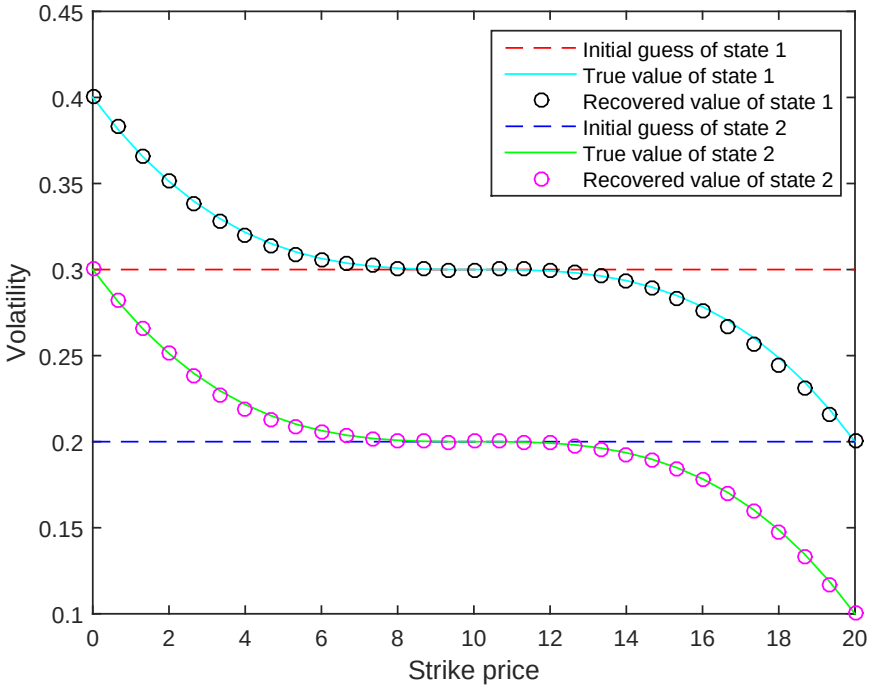


Figure 3: Recovery of the skew-shape volatility

Finally, our algorithm is also tested with the "skew" shape of volatility functions, because the graph for the volatility can be downward sloping for some markets (cf. Xing et al. (2010)), such as equity options. Hence, the volatility functions are selected as

$$\sigma_1(S) = 0.3 - \frac{(S-10)^3}{10000}, \quad \sigma_2(S) = 0.2 - \frac{(S-10)^3}{10000}, \tag{4.4}$$

and the results are given in Figure 3. Again, it is not difficult to find that the two skew volatility functions are also successfully recovered with the two flat initial guesses, and the errors are in the order of $10^{-4}$.

By testing the three typical kinds of volatility functions with different characteristics, we are confident to draw the conclusion that our algorithm can provide good recovery results for different shapes of volatility curves and it has the potential to be applied in real markets.

## 4.2 Stability test

Apart from the accuracy, another important factor associated with a newly derived numerical algorithm is its stability since there always exists noise in market prices. As a result, in order to demonstrate the stability of our algorithm, a white noise is added to the "true" volatility functions, and the procedure will be illustrated in the following. As an example, we consider the "smile" case used in the last subsection, and we further introduce two random variables, $x$ and $y$, both of which follow a standard normal distribution so that the noised "volatility" functions are specified as

$$\sigma_1(S) = [0.3 + \frac{(S-10)^2}{1000}](1 + \frac{x}{15}), \quad \sigma_2(S) = [0.2 + \frac{(S-10)^2}{1000}](1 + \frac{y}{15}). \tag{4.5}$$

Then, similar to the tests conducted in the last subsection, we use the noised "volatility" functions to generate state prices, which will be used as noised market state prices and recover volatility functions with our algorithm.

Depicted in Figure 4 are the recovery results with the generated noised state prices with initial guesses being flat lines. As expected, the recovered volatility functions from the noised state prices no longer fit very well to the un-noised "true" volatility functions as a direct result of introducing a white noise. However, it should be noted that this figure can clearly demonstrate the stability of our algorithm as the recovered volatility functions

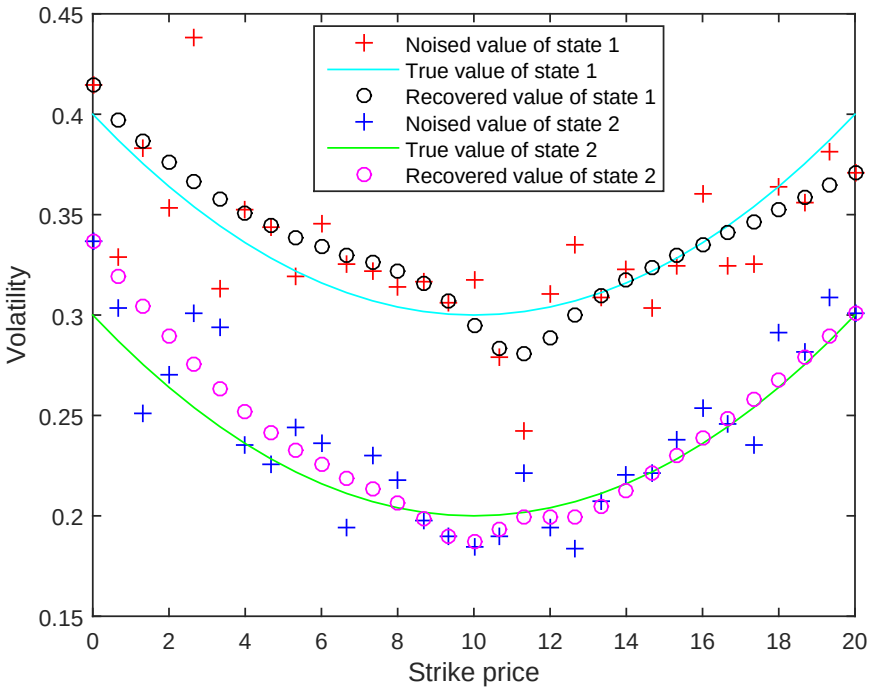


Figure 4: Stability test.

are still closely located around the un-noised "true" volatility functions.

## 4.3 Market tests

Having the accuracy and stability of the newly designed algorithm, we are now ready to test the performance of our algorithm with real market data, which adds another dimension of complexity due to an additional procedure that needs to be instrumented to overcome the difficulty that there are more needed state prices than the available market prices in the calibration of a regime-switching model as discussed in Section 2 already. Such difficulty did not arise in the tests presented in the previous two subsections at all because the state prices are generated with the "true" volatility functions. In other words, there was no need to determine the market-implied state prices, $C_1$ and $C_2$, in the previous tests, whereas they now need to be recovered from the market option prices in a real empirical test. This is achieved by calibrating the standard regime switching model to find $V_1$ and $V_2$ first and

then use Equation (2.3) and (2.4) to obtain $C_1$ and $C_2$ with a given market option price $C^{market}$.

Here, we use the market data of S&P 500 returns and options with prices quoted on 15 May 2013 and the expiry time of the options being 22 Jun 2013 (cf. CBOE (2017)). This means that the underlying price is $S_0 = 1658.78$, the expiry time $T = 0.1041$ (current time is 0), the risk-free interest rate (we use the LIBOR rate as an approximation) $r = 0.0027$, and the strike price ranges from 1120 to 1800 with $N_1 = 136$. By making use of one popular global optimization algorithm, Adaptive Simulated Annealing (cf. Ingber (2000), Mikhailov and Nögel (2004)), we obtain the estimated parameters as

$$\lambda_{12} = 0.2779,\ \lambda_{21} = 0.4355,\ \sigma_1 = 0.0495,\ \sigma_2 = 0.1160,\ \pi = 0.1520, \tag{4.6}$$

from which we can certainly get $V_1$ and $V_2$. In this way, we can obtain the two sets of market-implied state prices $C_1$ and $C_2$ with Equation (2.3) and (2.5).

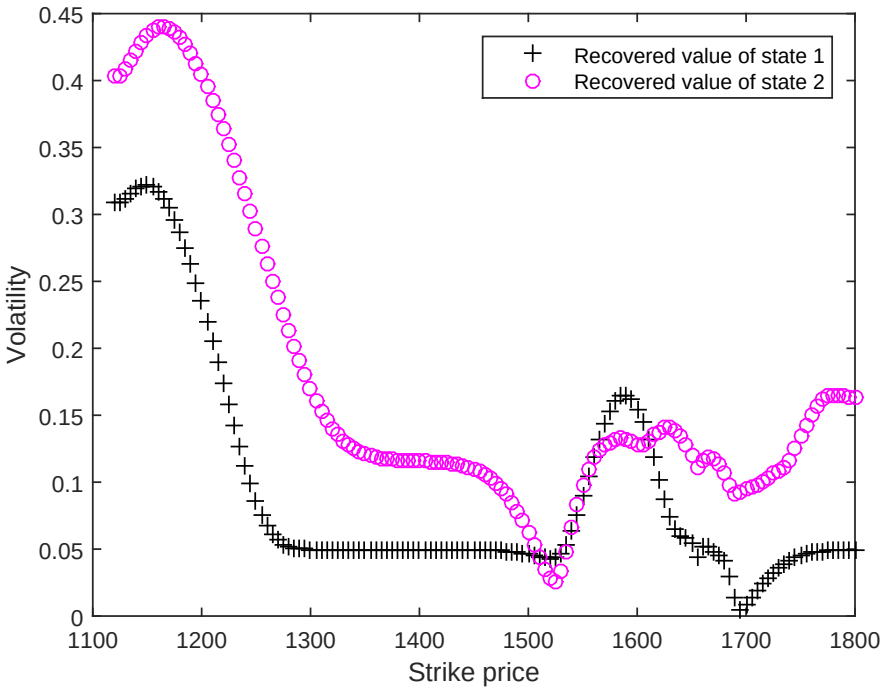


Figure 5: Market test.

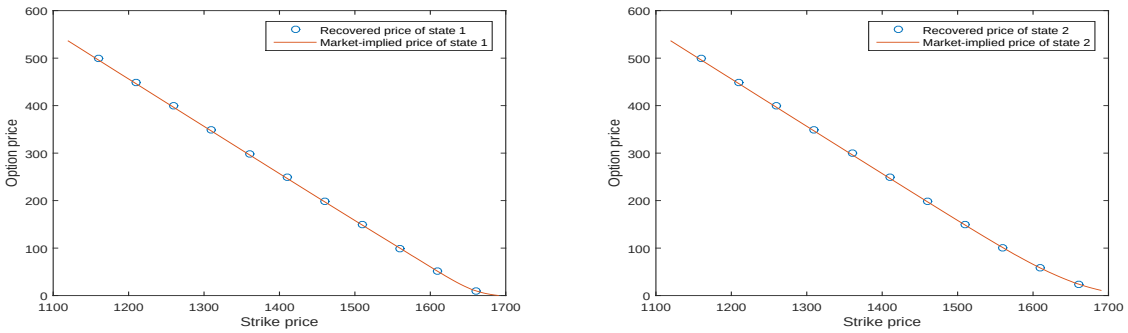


(a) State 1. (b) State 2.

Figure 6: Recovered price vs Market-implied price.

Having obtained the market-implied state prices, the remaining work is to recover local volatility functions with our algorithm, which is similar to what we have done in numerical tests. Parameters are set to be $N_2 = 20,\ \delta = 10^{-3} * S_0^2,\ \theta = 10^{-2},\ \epsilon = 10^{-9}$, and results are presented in Figure 5. It is clear that the level of the local volatility in State 1 is generally lower than that of State 2, and a roughly "smile" like shape can be observed for the two recovered volatility functions that the level of the volatility is relatively higher when the options is deep in-the-money and out-of-money while it is lower when the strike price is close to the underlying price. Moreover, it is interesting to notice that there are sudden jumps in the recovered local volatility functions when the strike price is close to the current index. On the other hand, to show whether we have recovered correctly recovered the two sets of market-implied state prices, we further show the option prices calculated with the recovered local volatility and those market-implied state prices in Figure 6. Obviously, with the maximum relative difference being 0.9%, our recovered results can certainly be regarded as accurate. From another prospective, the accuracy of our algorithm can also be demonstrated by comparing the implied volatility[2] extracted from market prices and that extracted from model prices (cf. Dai et al. (2016)), and the results are shown in Figure 7. As expected, the implied volatility exhibits a smile curve, and the implied volatility extracted from market prices agrees well with that extracted from model prices, with the

[2]Conventionally, implied volatility refers to that "implied" by the B-S model.

relative difference being no larger than 0.8%. A nearly perfect replication of the volatility smile exhibits the power of adopting a modern model, such as the regime-switching model, in option pricing.

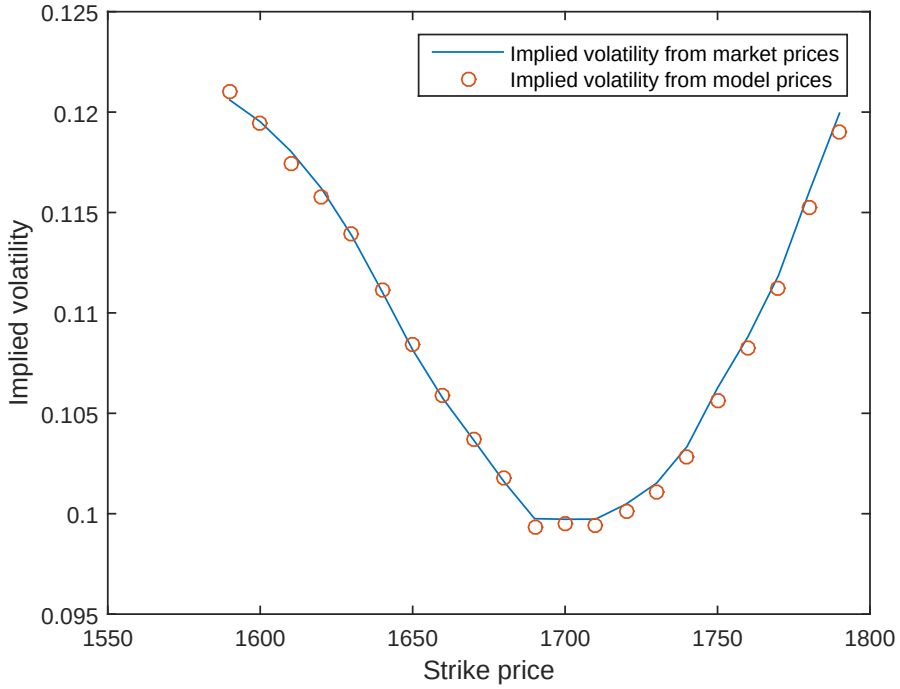


Figure 7: The comparison of implied volatility extracted from market prices and that from model prices.

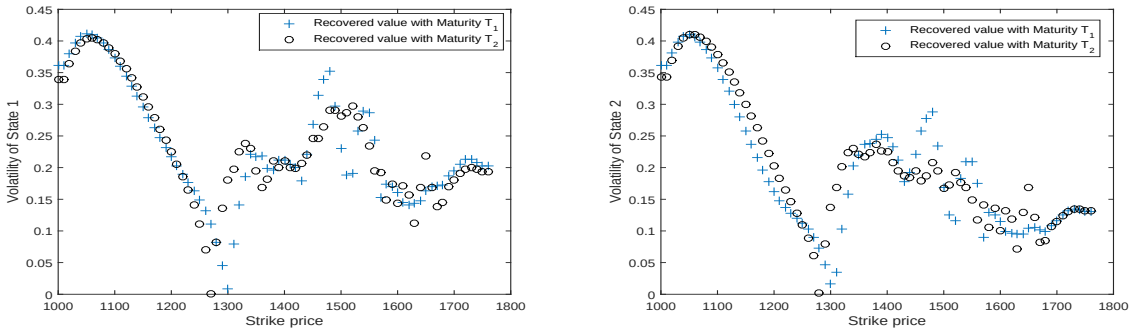


(a) State 1. (b) State 2.

Figure 8: Recovered volatility level with different maturities.

In order to focus on the core issue of this paper, i.e., to propose an appropriate approach for the calibration of a local regime-switching model, we have made a simplified assumption

in the illustration of the implementation of our approach that the local volatility functions is independent of time. Of course, in general, the local volatility function should depend on not only maturities but also strike prices. Naturally, one wonders if there are cases in finance practice where our simplified assumption can be justified[3]. To address this point, we need to use market option data with two different maturities and demonstrate that the recovered local volatility functions are insignificantly different. Such an exercise was conducted on a set of one-day option data (S&P 500 returns and options) with the prices quoted on 15 April 2013 and the two expiry times of the options being 22 June 2013 and 20 July 2013, respectively.

For this case, the underlying price is $S_0 = 1552.36$, the two expiry times, $T_1$ and $T_2$, take the value of 0.1863 and 0.2630, respectively. The risk-free interest rate $r$ is 0.0028 and the strike price ranges from 1000 to 1760 with $N_1 = 76$. Again, the first step of the calibration is to determine the market-implied state prices, $C_1$ and $C_2$, and thus we use Adaptive Simulated Annealing to obtain the estimated parameters as

$$\lambda_{12} = 0.4996,\ \lambda_{21} = 0.5010,\ \sigma_1 = 0.1826,\ \sigma_2 = 0.1222,\ \pi = 0.1222, \tag{4.7}$$

from which we can certainly obtain $V_1$ and $V_2$ as well as $C_1$ and $C_2$ through Equation (2.3) and (2.5) for each expiry time. With the market-implied state prices in hands, we are then able to recover the corresponding local volatility functions with our algorithm for different maturities, the results of which are presented in Figure 8. Apart from a slightly larger difference between the two recovered local volatility functions corresponding to the two maturities when the options are slightly in the money, the overall average absolute differences of the two recovered local volatility functions are very small. Specifically, the average absolute differences between the recovered volatility functions of the two maturities are 0.029 and 0.030 for State 1 and State 2 respectively. Of course, while the closeness of

[3]Note, even there was a couple of cases in which our assumption turns out to be a reasonable assumption, it does not mean that such an assumption can suit all market situations, as there are bound to be cases where the local volatility functions need to be assumed to vary with both maturities and strike prices.

the local volatility functions for two different maturities found in this particular example supports that our assumption may be reasonable in some cases, this does not mean that such an assumption should always be adopted in real markets in general.

# 5 Conclusion

In this paper, we present theoretical results on how to calibrate local regime-switching models. Although the Dupire-style formula for local regime-switching models has already been derived (cf. Elliott et al. (2015)), it is shown that this formula alone can not lead to final results as all the state prices are required whereas only one market price for an option is available in real markets. As a result, a closed system for option pricing and model calibration under the classical regime-switching model is firstly proposed with the market price being the expectation of state prices, based on which one market option price is successfully split into two market-implied state prices with a special approach. Upon noticing that the direct implementation of the Dupire formula with all state prices still can not yield accurate results, the calibration problem is formed as an inverse problem, which is further transformed into an optimal control problem due to its ill-posedness. With the use of Tikhonov regularization, two necessary conditions are derived for the existence of the optimal solution, and an efficient numerical algorithm is proposed for the recovery of local volatility functions. Finally, numerical experiments with synthetic data are carried out to demonstrate the accuracy and stability of our newly proposed algorithm. Interestingly, the local volatility functions recovered with real market data exhibits a smile-shape curve.

# References

Aı, Y., Kimmel, R. et al. (2007), 'Maximum likelihood estimation of stochastic volatility models', *Journal of Financial Economics* **83**(2), 413–452.

Bakshi, G., Cao, C. and Chen, Z. (1997), 'Empirical performance of alternative option pricing models', *The Journal of Finance* **52**(5), 2003–2049.

Bates, D. S. (2000), 'Post-'87 crash fears in the s&p 500 futures option market', *Journal of Econometrics* **94**(1), 181–238.

Black, F. and Scholes, M. (1973), 'The pricing of options and corporate liabilities', *The journal of political economy* pp. 637–654.

Bollen, N. P. (1998), 'Valuing options in regime-switching models', *The Journal of Derivatives* **6**(1), 38–49.

Bouchouev, I. and Isakov, V. (1997), 'The inverse problem of option pricing', *Inverse Problems* **13**(5), L11.

Buffington, J. and Elliott, R. J. (2002), 'American options with regime switching', *International Journal of Theoretical and Applied Finance* **5**(05), 497–514.

CBOE (2017), https://datashop.cboe.com/option-quotes-end-of-day-with-calcs. Accessed: 15/Feb/2017.

Chan, K. C., Karolyi, G. A., Longstaff, F. A. and Sanders, A. B. (1992), 'An empirical comparison of alternative models of the short-term interest rate', *The journal of finance* **47**(3), 1209–1227.

Chernov, M., Gallant, A. R., Ghysels, E. and Tauchen, G. (2003), 'Alternative models for stock price dynamics', *Journal of Econometrics* **116**(1), 225–257.

Choi, S.-Y., Fouque, J.-P. and Kim, J.-H. (2013), 'Option pricing under hybrid stochastic and local volatility', *Quantitative Finance* **13**(8), 1157–1165.

Coleman, T. F., Li, Y. and Verma, A. (2001), Reconstructing the unknown local volatility function, *in* 'Quantitative analysis in financial markets: collected papers of the New York University Mathematical Finance Seminar', Vol. 2, p. 192.

Crepey, S. (2003), 'Calibration of the local volatility in a generalized black–scholes model using tikhonov regularization', *SIAM Journal on Mathematical Analysis* **34**(5), 1183–1206.

Dai, M., Tang, L. and Yue, X. (2016), 'Calibration of stochastic volatility models: A tikhonov regularization approach', *Journal of Economic Dynamics and Control* **64**, 66–81.

De Cezaro, A., Scherzer, O. and Zubelli, J. (2012), 'Convex regularization of local volatility models from option prices: convergence analysis and rates', *Nonlinear Analysis: Theory, Methods & Applications* **75**(4), 2398–2415.

Derman, E. and Kani, I. (1994), 'Riding on a smile', *Risk* **7**(2), 32–39.

Derman, E., Kani, I. and Zou, J. Z. (1996), 'The local volatility surface: Unlocking the information in index option prices', *Financial analysts journal* **52**(4), 25–36.

Dumas, B., Fleming, J. and Whaley, R. E. (1998), 'Implied volatility functions: Empirical tests', *The Journal of Finance* **53**(6), 2059–2106.

Dupire, B. (1994), 'Pricing with a smile', *Risk* **7**(1), 18–20.

Egger, H. and Engl, H. W. (2005), 'Tikhonov regularization applied to the inverse problem of option pricing: convergence analysis and rates', *Inverse Problems* **21**(3), 1027.

Elliott, R. J., Chan, L. and Siu, T. K. (2015), 'A dupire equation for a regime-switching model', *International Journal of Theoretical and Applied Finance* **18**(04), 1550023.

Elliott, R. J., Kuen Siu, T. and Chan, L. (2007), 'Pricing volatility swaps under heston's stochastic volatility model with regime switching', *Applied Mathematical Finance* **14**(1), 41–62.

Eraker, B. (2004), 'Do stock prices and volatility jump? reconciling evidence from spot and option prices', *The Journal of Finance* **59**(3), 1367–1404.

Fengler, M. R., Härdle, W. K. and Villa, C. (2003), 'The dynamics of implied volatilities: A common principal components approach', *Review of Derivatives Research* **6**(3), 179–202.

Gatheral, J. (2011), *The volatility surface: a practitioner's guide*, Vol. 357, John Wiley & Sons.

Goutte, S. (2013), 'Pricing and hedging in stochastic volatility regime switching models', *Journal of Mathematical Finance* **3**(01), 70.

Hagan, P. S., Kumar, D., Lesniewski, A. S. and Woodward, D. E. (2002), 'Managing smile risk', *The Best of Wilmott* p. 249.

Hamilton, J. D. (1989), 'A new approach to the economic analysis of nonstationary time series and the business cycle', *Econometrica: Journal of the Econometric Society* pp. 357–384.

Hamilton, J. D. (1990), 'Analysis of time series subject to changes in regime', *Journal of econometrics* **45**(1), 39–70.

Heston, S. L. (1993), 'A closed-form solution for options with stochastic volatility with applications to bond and currency options', *Review of financial studies* **6**(2), 327–343.

Hofmann, B. and Krämer, R. (2005), 'On maximum entropy regularization for a specific inverse problem of option pricing', *Journal of Inverse and Ill-posed Problems jiip* **13**(1), 41–63.

Ingber, L. (2000), 'High-resolution path-integral development of financial options', *Physica A: Statistical Mechanics and its Applications* **283**(3), 529–558.

Janczura, J. and Weron, R. (2012), 'Efficient estimation of markov regime-switching models: An application to electricity spot prices', *AStA Advances in Statistical Analysis* **96**(3), 385–407.

Jiang, L., Chen, Q., Wang, L., Zhang, J. E. et al. (2003), 'A new well-posed algorithm to recover implied local volatility', *Quantitative Finance* **3**(6), 451–457.

Kamp, R. (2009), 'Local volatility modelling'.

Mikhailov, S. and Nögel, U. (2004), *Hestons stochastic volatility model: Implementation, calibration and some extensions*, John Wiley and Sons.

Mitra, S. and Date, P. (2010), 'Regime switching volatility calibration by the baum–welch method', *Journal of computational and applied mathematics* **234**(12), 3243–3260.

Musiela, M. and Rutkowski, M. (2006), *Martingale methods in financial modelling*, Vol. 36, Springer Science & Business Media.

Naik, V. (1993), 'Option valuation and hedging strategies with jumps in the volatility of asset returns', *The Journal of Finance* **48**(5), 1969–1984.

Rebonato, R. (2005), *Volatility and correlation: the perfect hedger and the fox*, John Wiley & Sons.

Rubinstein, M. (1994), 'Implied binomial trees', *The Journal of Finance* **49**(3), 771–818.

Scott, L. O. (1997), 'Pricing stock options in a jump-diffusion model with stochastic volatility and interest rates: Applications of fourier inversion methods', *Mathematical Finance* **7**(4), 413–426.

Siu, T. K., Yang, H. and Lau, J. W. (2008), 'Pricing currency options under two-factor markov-modulated stochastic volatility models', *Insurance: Mathematics and Economics* **43**(3), 295–302.

Tikhonov, A. N., Goncharsky, A., Stepanov, V. and Yagola, A. G. (2013), *Numerical methods for the solution of ill-posed problems*, Vol. 328, Springer Science & Business Media.

Van der Stoep, A. W., Grzelak, L. A. and Oosterlee, C. W. (2014), 'The heston stochastic-local volatility model: efficient monte carlo simulation', *International Journal of Theoretical and Applied Finance* **17**(07), 1450045.

Vogel, C. R. (2002), *Computational methods for inverse problems*, Vol. 23, Siam.

Xing, Y., Zhang, X. and Zhao, R. (2010), 'What does the individual option volatility smirk tell us about future equity returns?'.

Yen, J. and Lai, K. K. (2014), *Emerging Financial Derivatives: Understanding Exotic Options and Structured Products*, Routledge.

Zhu, S.-P., Badran, A. and Lu, X. (2012), 'A new exact solution for pricing european options in a two-state regime-switching economy', *Computers & Mathematics with Applications* **64**(8), 2744–2755.